Current plate motion across the Dead Sea Fault from three years of continuous GPS monitoring

Shachak Pe'eri, Shimon Wdowinski, Alon Shtibelman, and Noa Bechor
Department of Geophysics and Planetary Sciences, Tel-Aviv University, Ramat-Aviv, Israel

Yehuda Bock, Rosanne Nikolaidis, and Matthijs van Domselaar
Institute of Geophysics and Planetary Physics, Scripps Institution of Oceanography, University of California, San Diego, USA

Received 3 August 2001; revised 19 December 2001; accepted 3 January 2002; published 26 July 2002.

[1] The Dead Sea Fault (DSF) is a transform plate boundary between the Arabian plate and the Sinai sub-plate. The rate of displacement across the fault has been estimated as 1–10 mm/yr. In this study we present a new estimate of the current displacement across the DSF, which is based on three years of continuous Global Positioning System measurements (July 1996 to July 1999). Our analysis of these data shows that relative northward velocity, which is the fault parallel component, on the baseline between Tel Aviv and Katzerin (Golan Heights) and Katzerin and Elat is 1.4 ± 0.3 mm/yr and −1.0 ± 0.5 mm/yr, respectively, assuming a colored noise (white noise plus flicker noise) model for the daily position estimates. By using a simple locked fault model, we estimate that during the three-year observation period the relative plate motion across the DSF was 2.6 ± 1.1 mm/yr. *INDEX TERMS:* 8158 Tectonophysics: Evolution of the Earth: Plate motions—present and recent (3040); 8150 Tectonophysics: Evolution of the Earth: Plate boundary—general (3040); 8107 Tectonophysics: Continental neotectonics; 1243 Geodesy and Gravity: Space geodetic surveys

1. Introduction

[2] The eastern Mediterranean consists of three major plates, Arabia, Nubia and Eurasia, and two sub-plates, Anatolia and Sinai. In the Levant area (Figure 1), these plates are separated by a series of faults that evolved after the separation of the once united Nubian-Arabian plate [*Freund et al.*, 1970]. One of the main faults, the Dead Sea Fault (DSF), is a transform plate boundary separating the Sinai sub-plate from the Arabian plate [*Quennell*, 1959; *Wilson*, 1965]. Its length exceeds 1000 km, linking the Zagros-Taurus convergence zone with the diverging zone of the Red Sea. The DSF was formed in the early Miocene [*Garfunkel*, 1981]. The total displacement across the fault is 80–105 km, in which the larger displacement has been detected along the southern part of the fault (south of N32°) [*Garfunkel*, 1981]. The relative motion across the DSF has been estimated by a variety of methods, including geological, geophysical (seismic) and paleoseismological techniques. Overall the relative plate motion has been estimated to be in the range of 1–10 mm/yr, depending on the timescale of the observations.

0094-8276/02/2001GL013879$05.00

[3] This study presents a new estimate of the current plate motion across the DSF obtained from three years of continuous GPS (CGPS) observations (July 1996 to July 1999) from the first three such stations in Israel. Previous survey mode measurements of the Galilee-Golan network, conducted during the years 1990–1993, measured no significant motion across the northern section of the DSF [*Adler et al.*, 1994]. However, CGPS observations provide more accurate velocity measurements [*Zhang et al.*, 1997].

2. Observations

[4] As part of the growing space geodetic activity in Israel, the Survey of Israel installed in 1996–1997 three CGPS stations in Tel Aviv, Katzerin (Golan Heights) and Elat (Figure 1, Table 1). The stations were constructed on roofs of stable buildings mainly for geodetic purposes, i.e., to provide infrastructure for precise geodetic measurements in Israel, but also for monitoring current crustal movements along the DSF. Since 1998 these three stations have been integrated into the 12-station GIL ("GPS in Israel") network, which provides GPS infrastructure for a variety of geodetic applications and geophysical research in Israel [*Wdowinski et al.*, 2001].

[5] The station locations were chosen according to both geodetic and geodynamic considerations, as well as political constraints. Two of the stations are located west of the fault; one lies within the fault zone (ELAT) and the other lies 70 km west of the fault (TELA), within the tectonically stable part of the Sinai sub-plate. The third station (KATZ) is located 5.5 km east of the fault and also lies within the fault deformation zone. Due to the lack of stations in the stable part of the Arabian plate, the station distribution does not allow us to measure directly the total plate motion across the DSF. Nevertheless, it is still possible to measure plate boundary deformation, from which the full plate motion can be inferred.

[6] The three CGPS stations used in this study are equipped with geodetic-quality GPS receivers and antennas (Trimble SSE units), power supplies, dedicated telephone lines, and modems. Data collection is performed in 24 hour segments ($0–24^h$ UTC). The receivers record at a 30 s sampling rate. The GPS data for all GIL stations are downloaded daily to data collection centers at Tel Aviv University and the Survey of Israel and are translated to the Receiver Independent Exchange format (RINEX). The daily RINEX files are archived at Tel Aviv University and are

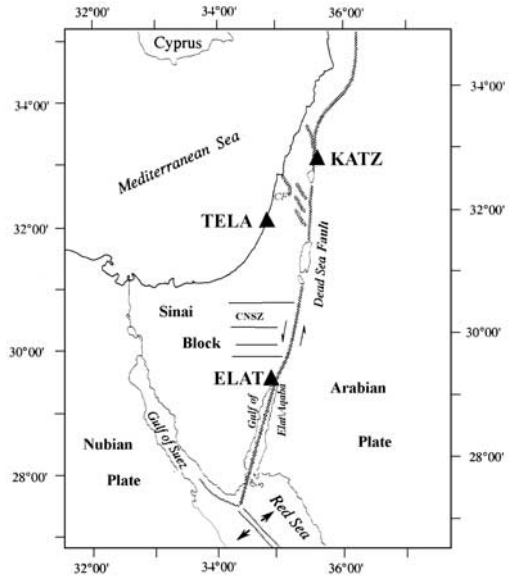

Figure 1. Tectonic map of the Levant showing the main fault systems separating the Sinai sub-plate and the Arabian plate. Solid triangles denote the locations of the three CGPS stations in Israel. CF and CNSZ denote the Carmel Fault and Central Negev Shear Zone, respectively.

available to all users via anonymous ftp (tecton.tau.ac.il) or the Internet (http://www.tau.ac.il/~shimonw/gps), and at the Scripps Orbit and Permanent Array Center (SOPAC, ftp://garner.ucsd.edu; http://sopac.ucsd.edu).

3. Data Analysis and Results

[7] The GPS measurements were analyzed in a three-step procedure using the GAMIT/GLOBK software packages [*King and Bock*, 2000; *Herring*, 2000]. In the first step, daily GAMIT/GLOBK analyses of the global IGS network, consisting of 80–120 CGPS stations, were conducted with loose constraints to calculate precise orbits and Earth orientation parameters (EOP). In the second stage, the calculated orbits and EOP were used with tight constraints in daily GAMIT/GLOBK analyses of the 3 stations and the 10–14 nearest IGS stations, solving for daily average three-dimensional station positions. In the third stage, a GLOBK analysis of all daily global and regional solutions was conducted to align all calculated station positions in the IGS97 reference frame [*Ferland et al.*, 2000].

[8] We choose to present our results as baseline time series and not single-station positioning (e.g., as used by *Bock et al.* [1997]), because the velocity differences between the three stations are very small. Figure 2 shows three-dimensional time series of baseline positions between the three CGPS stations used in this study. The longest time series of 36 months (July 1996–July 1999) is obtained for the KATZ-TELA baseline. Because the ELAT station was established only in 1997 (Table 1), the two other series are only 30 months long.

Table 1. List of the GPS Stations and their Geographic Location

Code	Name	Geographic Coordinates	
KATZ	Katzerin	N 32°49′	E 35°41′
TELA	Tel Aviv	N 31°53′	E 34°46′
ELAT	Elat	N 29°20′	E 34°55′

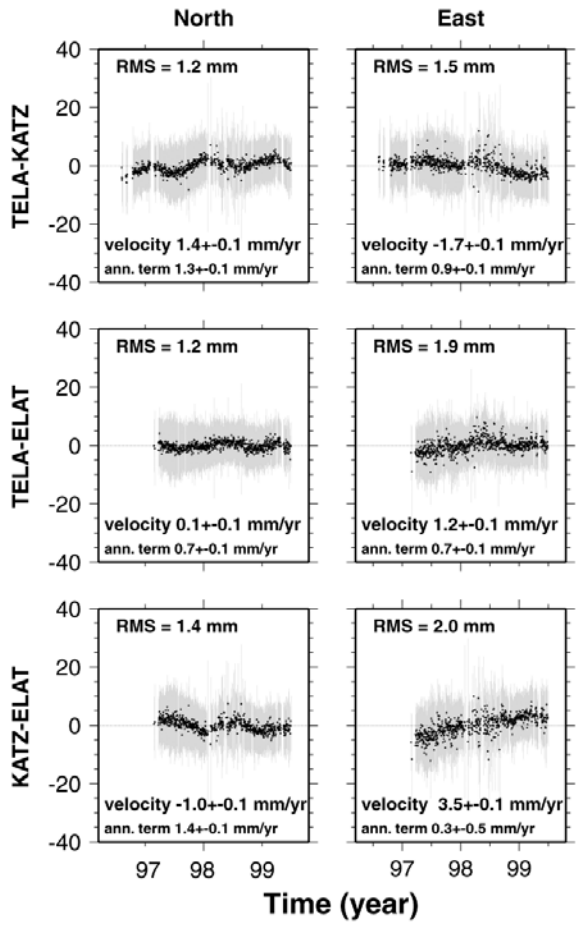

Figure 2. Three-year time series of the relative positions (mm) between Tel Aviv, Katzerin and Elat stations. Daily relative positioning (with respect to an average value) are marked by black dots and their 1-σ uncertainties are shown by gray error bars.

[9] We estimated four parameters for each baseline time series; an offset, a slope (velocity) and amplitude and phase terms of an annual signal, assuming a white noise model for the observations (i.e., the daily baseline positions). First, we removed a small number of outliers defined by three times the interquartile range of the data (e.g., as used by *Bock et al.* [2000]). The quality of the estimated daily positions is best quantified by the repeatability (root mean square - RMS) of the modeled time series. Figure 2 shows that the repeatabilities in relative position are 1.2–1.4 mm for the north component, 1.5–2.0 mm for the east component, and 5–6 mm for the vertical component. The estimated velocities have a (one-sigma) uncertainty of about 0.1 mm/yr in the horizontal component and 0.3 mm/yr in the vertical component (Table 2). After accounting for colored noise in the baseline time series (i.e., by scaling the uncertainties by a conservative factor of 6 according to the white noise plus flicker noise model shown in Figure 7 of *Zhang et al.* [1997]), the estimated horizontal velocities are significant at the 95% confidence level, while the vertical velocities

Table 2. Observed Baseline Velocities as Determined with 1-σ Uncertainties (mm/yr) Assuming a White Noise Model for the Daily Baseline Estimates

Baseline	North	East	Vertical
TELA-KATZ	1.40 ± 0.05	−1.74 ± 0.07	−0.56 ± 0.21
TELA-ELAT	0.13 ± 0.07	1.17 ± 0.12	1.18 ± 0.31
KATZ-ELAT	−1.00 ± 0.08	3.52 ± 0.12	0.90 ± 0.37

ranging from only 0.6–1.2 mm/yr are not significantly different from zero velocity.

4. Discussion and Conclusions

[10] The analysis of three years of data (of the three CGPS stations in Israel - Tel Aviv, Katzerin, and Elat) shows that the current crustal movements between the stations are very slow, 1–4 mm/yr (Figure 2, Table 2). In order to evaluate the tectonic significance of the observed velocities, we analyze them with respect to the main tectonic element in the region, the DSF, which is oriented in a N-S direction, using a deformable plate boundary model. The model considers interseismic deformation along active faults, which takes place between major earthquakes (coseismic deformation). According to the model, the relative motion between the stations reflect only a portion of the full plate motion, because the KATZ and ELAT stations are located very close to the fault (Table 3), within the elastically deforming plate boundary region. Thus, the observed N-S 1.0–1.4 mm/yr relative northward motion, which represents the fault parallel component, roughly reflects half of the total plate motion across the DSF; a detailed analysis of our estimate is given below.

[11] The observed E-W motion between the stations cannot be explained by our simple model, which accounts only for N-S movements. The observed 1.7–3.5 mm/yr E-W motion reflects left-lateral shear component, which is consistent with the sense of motion along NW-SE trending Carmel Fault [*Ron et al.*, 1984] in northern Israel, but contradicts the geological determined right-lateral motion along the Central Negev Shear Zone in southern Israel (Figure 1). However, the large E-W velocity of ELAT, with respect to both stations, may reflect a remnant postseismic deformation caused by the 1995 Nuweiba earthquake, whose epicenter was located 80 km south of ELAT [*Baer et al.*, 1999].

[12] A quantitative estimate for the full plate motion across the DSF is derived using the locked-fault model of *Savage and Burford* [1973] for an infinitely long fault (Figure 3a). We use this model because it is simple and depends only on three parameters. The model assumes a half-space that consists of an upper elastic seismogenic layer of a uniform thickness (D) overlying two blocks sliding horizontally past each other at a constant velocity

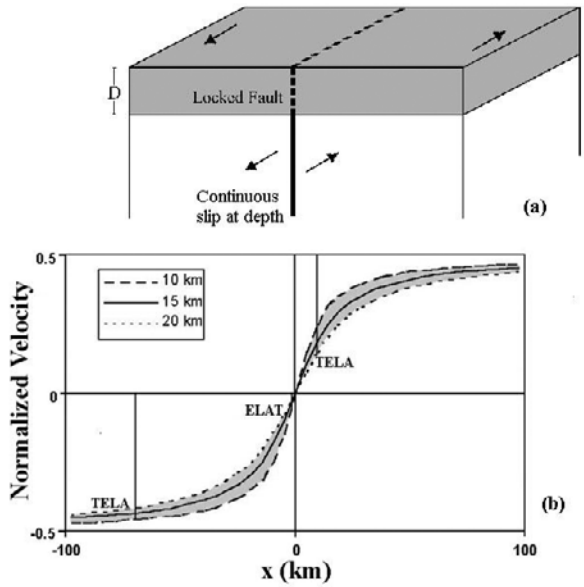

Figure 3. (a) A schematic illustration of a locked-fault model. (b) Graphical illustration of the surface velocity $V(x)$ as a function of the distance from the fault calculated by the locked-fault model using 10, 15, and 20 km locking depths (D). The velocity is normalized by respect to the relative plate motion (V_0).

(V_0). We assume an infinitely long fault, in order to obtain a very simple model that can be constrained by our limited number of data. This assumption implies that the velocity of the fault-normal component reduces to zero, whereas the velocity of the fault-parallel component at the surface depends only on the horizontal distance from the fault (x). The mathematical description of the surface normalized fault-parallel velocity is

$$\frac{V(x)}{V_0} = \frac{1}{\pi}\arctan\left(\frac{x}{D}\right) \quad (1)$$

which is shown in Figure 3b. We use the normalized form, because the sliding velocity (V_0), which is also the full plate motion, is unknown. The sliding velocity is estimated using the observed north components of the baselines KATZ-TELA and ELAT-TELA, which fortunately almost coincide with the fault parallel movements along the predominantly N-S oriented DSF (Figure 1).

Table 3. Modeled Normalized Velocity, as Calculated for the Three Sites with 10, 15 and 20 km Thickness Seismogenic Layer (D)

Site	Location wrt the DSF - x (km)	Modeled Normalized Velocity $V(x)/V_0$		
		D = 10 km	D = 15 km	D = 20 km
KATZ	5.5	0.16	0.11	0.09
TELA	−70	−0.46	−0.44	−0.42
ELAT	−1.5	−0.05	−0.04	−0.03

Table 4. Observed and Modeled Baseline Velocities Used for Calculating the Full Relative Plate Motion (v_0) Across the DSF

Baseline	Observed Velocity (mm/yr) ΔV_{Obs}	Modeled Velocity (normalized) $\Delta V_{Mod}/V_0$	Calculated relative plate motion (mm/yr) $V_0 = \Delta V_{obs}/(\Delta V_{Mod}/V_0)$
TELA-KATZ	1.40 ± 0.30	0.51–0.62	2.6 ± 0.8
TELA-ELAT	0.13 ± 0.42	0.12–0.21	0.8 ± 4.0
KATZ-ELAT	−1.00 ± 0.48	−(0.39–0.41)	2.5 ± 1.3

The velocity uncertainties are determined by scaling the one-sigma white noise uncertainty (Table 2) by a conservative factor of 6, to account for the white noise plus flicker noise characteristic of continuous GPS time series [*Zhang et al.*, 1997; *Nikolaidis*, 2002].

[13] Estimating the full plate motion from the model and the observed baseline velocities requires several steps. First, we evaluate the predicted normalized velocity at the three sites according to their distance from the fault (Table 3). Because the fault locking depth (D) is poorly constrained, we evaluate the normalized velocities for a range of physically reasonable depths (Table 3, Figure 3b), as known from other strike-slip faults and from the nucleation depth of large and moderate earthquakes along the DSF. Second, we evaluate the normalized baseline velocities by subtracting the normalized site velocities one from the other, for each locking depth. Table 4 shows that the fault-parallel velocity component of baseline KATZ-TELA reflects 50–60% of the full plate motion, the ELAT-TELA velocity reflects 40%, and the KATZ-ELAT only 10–20% of the full motion. Third, for each baseline we evaluate the sliding velocity (V_0), which is the full plate motion, by dividing the observed baseline velocity by the normalized velocity (Table 4). Finally, we used a weighted average scheme to determine that the full plate motion between Sinai and Arabia is 2.6 ± 1.1 mm/yr.

[14] The GPS-based estimate of current plate motion across the DSF can be compared with other estimates, obtained using geologic, geomorphic, seismic, and historic data. Our 2.6 ± 1.1 mm/yr estimate is in agreement with the 4 ± 2 mm/yr rate of *Klinger et al.* [2000a, 2000b], who measured offset gullies in the Arava valley to calculate the average displacement rate for the past millennium [*Klinger et al.*, 2000b] and past 77–140 Kyr [*Klinger et al.*, 2000a]. Our estimate is also compatible with the 3–7.5 mm/yr rate of *Ginat et al.* [1998], who derived their estimate from translocated Pliocene drainage systems also located in the Arava valley. Our estimate also agrees with the 1–3.5 mm/yr short-term seismic and historic estimates [e.g., *Ben Menahem and Aboodi*, 1981; *Salomon*, 1993]. However, our estimate is significantly lower than the 6–10 mm/yr estimated from long-term geologic observations [e.g., *Joffe and Garfunkel*, 1987]. Nevertheless, recent geological data from the northern part of the DSF suggest that geologically derived rate was overestimated by a few tens of percent [*Garfunkel*, personal communication, 2000].

[15] The geodetically observed crustal movements along the DSF and their derived estimate of the current relative plate motion have significant implications for seismic hazard assessments for the Levant region. Our observations demonstrate that the DSF plate boundary region deforms and hence accumulates elastic strain, which eventually will be released by earthquakes. However, the new geodetic result should be considered very carefully because it relies on limited data and on a very simple modeling scheme. Furthermore, not all the observed motion necessarily reflects interseismic movement along the DSF; it may be contaminated by postseismic deformation, as suggested by the large eastward motion of ELAT, by interseismic deformation along secondary faults, or by anelastic deformation. Despite these limitations our results provides the first geodetic estimate of the current plate motion across the DSF. Further ongoing collection, processing and analysis of data from these three CGPS stations, as well as from the rest of the GIL network stations will provide a more detailed description of the current deformation pattern along the DSF.

[16] **Acknowledgments.** We thank the Survey of Israel, in particular Yosef Forrai and Yossi Melzer, for providing us with the CGPS data. We are thankful to two anonymous reviewers for their helpful comments. This study was funded by the Israel Space Agency.

References

Adler, R, H. Pelzer, K. Foppe, and Y. Melzer, Geodetic Monitoring of Recent Crustal Activity along the Dead Sea Jordan Rift, *Perelmuter Workshop on Dynamic Deformation Models*, Haifa, Israel, 1994.

Baer, G., D. Sandwell, S. Williams, and Y. Bock, Coseismic deformation associated with the November 1995, Mw = 7.1 Nuweiba earthquake, Gulf of Elat (Aqaba), detected by synthetic aperture radar interferometry, *Journal of Geophysical Research*, *104*, 25,221–25,232, 1999.

Ben Menahem, A., and E. Aboodi, Micro- and macroseismicity of the Dead Sea Rift and off-coast eastern Mediterranean, *Tectonophysics*, *80*, 199–233, 1981.

Bock, Y., S. Wdowinski, P. Fang, J. Zhang, J. Behr, J. Genrich, D. Agnew, F. Wyatt, H. Johnson, K. Hudnut, K. Stark, S. Dinardo, W. Young, and W. Gurtner, Southern California Permanent GPS Geodetic Array: Continuous measurements of crustal deformation, *J. Geophys. Res.*, *102*, 18,013–18,034, 1997.

Bock, Y., R. Nikolaidis, P. J. de Jonge, and M. Bevis, Instantaneous geodetic positioning at medium distances with the Global Positioning System, *J. Geophys. Res.*, *105*, 28,223–28,254, 2000.

Ferland, R., J. Kouba, and D. Hutchison, Analysis methodology and recent results of the IGS network combination, *Earth Planet Space*, *52*, 953–957, 2000.

Freund, R., Z. Garfunkel, I. Zak, M. Goldberg, T. Weisbrod, and B. Derin, The shear along the Dead Sea Rift, *Philo. Trans. R. Soc. London, Ser. A*, *267*, 107–130, 1970.

Garfunkel, Z., Internal structure of the Dead Sea leaky transform (Rift) in relation to plate kinematics, *Tectonophysics*, *80*, 81–108, 1981.

Ginat, H., T. Enzel, and Y. Avni, Translocated Plio-Pleistocene drainage systems along the Arava fault of the Dead Sea transform, *Tectonophysics*, *284*, 151–160, 1998.

Herring, T. A., Documentation of the GLOBK Software v. 5.04, Mass. Inst. of Technology, 2000.

Joffe, S., and Z. Garfunkel, Plate kinematics of the circum Red Sea – a re-evaluation, *Tectonophysics*, *141*, 5–22, 1987.

King, R.W., and Y. Bock, Documentation of the GAMIT GPS Analysis Software v. 9.9, Massachusetts Institute of Technology and Scripps Institution of Oceanography, 2000.

Klinger, Y., J. P. Avouac, N. Abou Karaki, L. Dorbath, D. Bourles, and J. L. Reyss, Slip rate on the Dead Sea transform fault in northern Araba valley (Jordan), *Geophys. J. Int.*, *142*, 755–768, 2000a.

Klinger, Y., J. P. Avouac, L. Dorbath, N. Abou Karaki, and N. Tisnerat, Seismic behaviour of the Dead Sea fault along Araba valley, *Geophys. J. Int.*, *142*, 769–782, 2000b.

Nikolaidis, R., Observation of Geodetic and Seismic Deformation with the Global Positioning System, PhD thesis, Scripps Institution of Oceanography, 2002.

Quennell, A. M., Tectonics of the Dead Sea Rift. *Int. Geol. Congr., 20th, Mexico, 1956- Assoc. Serv. Geol. Afr.*, 385–405, 1959.

Ron, H., R. Freund, Z. Garfunkel, and A. Nur, Block rotation by strike slip faulting: structural and paleomagnetic evidence, *Journal of Geophysical Research*, *89*, 6256–6270, 1984.

Salomon, A., Seismotectonic analysis of earthquakes in Israel and adjacent Areas. Ph.D. thesis, Hebrew University, Jerusalem, Israel, 1993.

Savage, J. C., and R. O. Burford, Geodetic determination of relative plate motion in Central California, *Jour. Geophys. Res.*, *78*, 832–845, 1973.

Wdowinski, S., Y. Bock, Y. Forrai, Y. Melzer, E. Ostrovsky, G. Baer, and D. Levitte, The GIL network of continuous GPS monitoring in Israel for geodetic and geophysical applications, *Isr. J. Earth Sci.*, *50*, 39–47, 2001.

Wilson, J. T., A New class of faults and their bearing on the continental drift, *Nature*, *207*, 343–347, 1965.

Zhang, J., Y. Bock, H. Johnson, P. Fang, S. Wdowinski, J. Genrich, and J. Behr, Southern California Permanent GPS geodetic array: Error analysis of daily position estimates and site velocities, *J. Geophys. Res.*, *102*, 18,035–18,056, 1997.

S. Pe'eri, S. Wdowinski, A. Shtibelman, and N. Bechor, Department of Geophysics and Planetary Sciences, Tel-Aviv University, Ramat-Aviv, Israel.

Y. Bock, R. Nikolaidis, and M. Van-Domselaar, Institute of Geophysics and Planetary Physics, Scripps Institution of Oceanography, University of California, San Diego, USA.